



Experimental Research on Electrical Conductivity of the Olivine-Ilmenite System at High Temperatures and High Pressures

Wenqing Sun¹, Lidong Dai^{1*}, Haiying Hu^{1*}, Mengqi Wang^{1,2}, Ziming Hu^{1,2} and Chenxin Jing^{1,2}

¹Key Laboratory of High-Temperature and High-Pressure Study of the Earth's Interior, Institute of Geochemistry, Chinese Academy of Sciences, Guiyang, China, ²University of Chinese Academy of Sciences, Beijing, China

OPEN ACCESS

Edited by:

Zhicheng Jing,
Southern University of Science and
Technology, China

Reviewed by:

George Amulele,
Case Western Reserve University,
United States
Xiaozhi Yang,
Nanjing University, China

*Correspondence:

Lidong Dai
dailidong@vip.gyig.ac.cn
Haiying Hu
huhaiying@vip.gyig.ac.cn

Specialty section:

This article was submitted to
Earth and Planetary Materials,
a section of the journal
Frontiers in Earth Science

Received: 24 January 2022

Accepted: 10 March 2022

Published: 05 April 2022

Citation:

Sun W, Dai L, Hu H, Wang M, Hu Z and
Jing C (2022) Experimental Research
on Electrical Conductivity of the
Olivine-Ilmenite System at High
Temperatures and High Pressures.
Front. Earth Sci. 10:861003.
doi: 10.3389/feart.2022.861003

Ilmenite is a common metallic oxide distributed in the mafic rocks from the Earth's upper mantle, and thus the effect of ilmenite contents on the electrical structures of the Earth's upper mantle should be investigated in detail. Electrical conductivities of the olivine-ilmenite systems with various contents of ilmenite ($V_{\text{ilm}} = 4, 7, 10, 11$ and 15 vol%) and pure ilmenite aggregates were measured using a complex impedance spectroscopic technique at $1.0\text{--}3.0$ GPa and $773\text{--}1273$ K. Electrical conductivities of the olivine-ilmenite systems increased with increasing temperatures in different degrees, conforming to the Arrhenius law. With the rise of pressure, the conductivities of the olivine-ilmenite systems slightly increased. According to the significant change of the conductivities, the percolation threshold of ilmenite grains in the olivine-ilmenite systems was proposed to be ~ 11 vol%. Isolated ilmenites moderately influence the conductivities of olivine aggregates, but the interconnected ilmenites dramatically enhanced the conductivities of the olivine-ilmenite systems. The conductivities of the olivine aggregates with 11 vol% ilmenites were about $1.5\text{--}3$ orders magnitude higher than those of 10 vol% ilmenites-bearing olivine aggregates. Small polarons were proposed to be the dominant charge carriers for olivine aggregates with isolated ilmenites (activation enthalpies: $0.62\text{--}0.89$ eV) and interconnected ilmenites (activation enthalpies: $0.15\text{--}0.20$ eV). Furthermore, the conductivity-depth profiles of olivine-ilmenite systems in the Earth's upper mantle were constructed, providing an important constraint on the electrical structures of the Earth's interior.

Keywords: electrical conductivity, olivine-ilmenite system, high pressure, conduction mechanism, mantle

INTRODUCTION

Electrical conductivity research for geological materials at high temperatures and pressures is a significant window to watch into the material compositions and thermodynamic state in the interior of the planets. Previous studies on the electrical conductivity were focused on the dominant silicate minerals and rocks, aqueous fluids, and silicate and carbonate melts in the Earth's interior (Huang et al., 2005; Ni et al., 2011; Yang et al., 2012; Dai et al., 2018; Guo et al., 2018; Guo and Keppler, 2019; Huang et al., 2021). It was proposed that the high conductivity anomalies in the Earth's interior can be caused by the various high-conductivity phases (e.g., melts, fluids, hydrogen in the nominally anhydrous minerals) (Wannamaker et al., 2009; Ni et al., 2011; Dai and Karato, 2014; Manthilake

et al., 2016; Laumonier et al., 2017; Sun et al., 2017; Guo et al., 2018; Li et al., 2018), and high-conductivity mineral phases (e.g., graphite, magnetite, iron sulfide) were determined to be one significant influence factor for the high conductivity anomalies (Watson et al., 2010; Wang et al., 2013; Zhang and Pommier, 2017). It is noted that the graphite is stable in the cratonic lithospheric mantle (Pearson et al., 1994), and aqueous fluids and melts are widely distributed in the subduction zones (Iwamori, 1998; Scambelluri and Philippot, 2001; Gaillard, 2005; Gaillard et al., 2008). A small quantity of high-conductivity minerals can dramatically enhance the conductivities of polycrystalline olivine (Wang et al., 2013; Zhang and Pommier, 2017; Dai et al., 2019). And thus, the high-conductivity minerals might play a significant role on the electrical structures of the Earth's upper mantle, where the most dominant mineral is olivine.

Ilmenites as mineral inclusions and accessory minerals are widely distributed in the peridotites and kimberlites in various geological regions (Ponomarenko, 1977; Risold et al., 2003; Wirth and Matsyuk, 2005; Pang et al., 2008; Cao et al., 2019), and exsolution of ilmenite from olivine is a common phenomenon (Liu et al., 2005; Massonne and Neuser, 2005). Due to the magmatic fractionation and crystallization, Ilmenite ore deposit can be formed in some special regions, such as Emeishan Large Igneous Province (She et al., 2015). It was implied that ilmenite exist in the interior of the Earth, and ilmenite contents of mafic rocks in various regions might be different. Ilmenites might be enriched in some peridotites of the special regions due to magmatic fractionations and crystallizations in the period of crust-mantle differentiation. In order to in-depth study electrical structures in the Earth's upper mantle, the influence of ilmenite contents on the olivine aggregates should be considered. Previous studies have researched the conductivities of monocrystalline olivine, olivine aggregates and olivine aggregates mixed with graphite, magnetite or metal sulfide (Dai et al., 2010; Wang et al., 2013; Dai and Karato, 2014; Zhang and Pommier, 2017; Dai et al., 2019). Single crystal of hydrous olivine shows the apparent anisotropy of electrical property, and the conductivity of olivine along the crystal orientation of [100], [010] and [001] decreases in order (Dai and Karato, 2014). In addition, water and iron contents significantly enhance the conductivity of olivine, providing a basis for the interpretation of electrical conductivity model of other planets with different iron and hydrogen contents (Dai and Karato, 2014). In the real geological environments, the material compositions of the Earth's interior are complicated, and change with spatial location. It was confirmed that olivine usually coexists with various contents of high-conductivity mineral phases (e.g., graphite, magnetite, et al.) in some special regions of the Earth's interior (Duba and Shankland, 1982; Yamanaka et al., 2001). When the concentration of graphite exceeds percolation threshold (~ 1 wt%), the conductivities of olivine aggregates with graphite was markedly enhanced (Wang et al., 2013). A small quantity of magnetite can also moderately enhance the conductivities of olivine aggregates (Dai et al., 2019). For the olivine-metal systems, the conductivities increased with the increase of metal: olivine

ratios and the contents of metal melt infiltrated into polycrystalline olivine matrix (Zhang and Pommier, 2017). However, electrical conductivities of olivine aggregates mixed with various contents of ilmenites at high temperatures and high pressures have not been investigated.

In the present study, we *in-situ* measured the conductivities of the dry olivine-ilmenite systems under the conditions of 1.0–3.0 GPa and 773–1273 K. Effects of temperature, pressure and ilmenite content on the conductivities of the olivine-ilmenite systems were systematically researched, and the conduction mechanism for the olivine-ilmenite systems was discussed in detail. According to the thermal models of the Earth's interior and electrical conductivity-temperature data of olivine aggregates with various contents of ilmenites, we constructed the electrical conductivity-depth profiles for the olivine-ilmenite systems in the Earth's upper mantles.

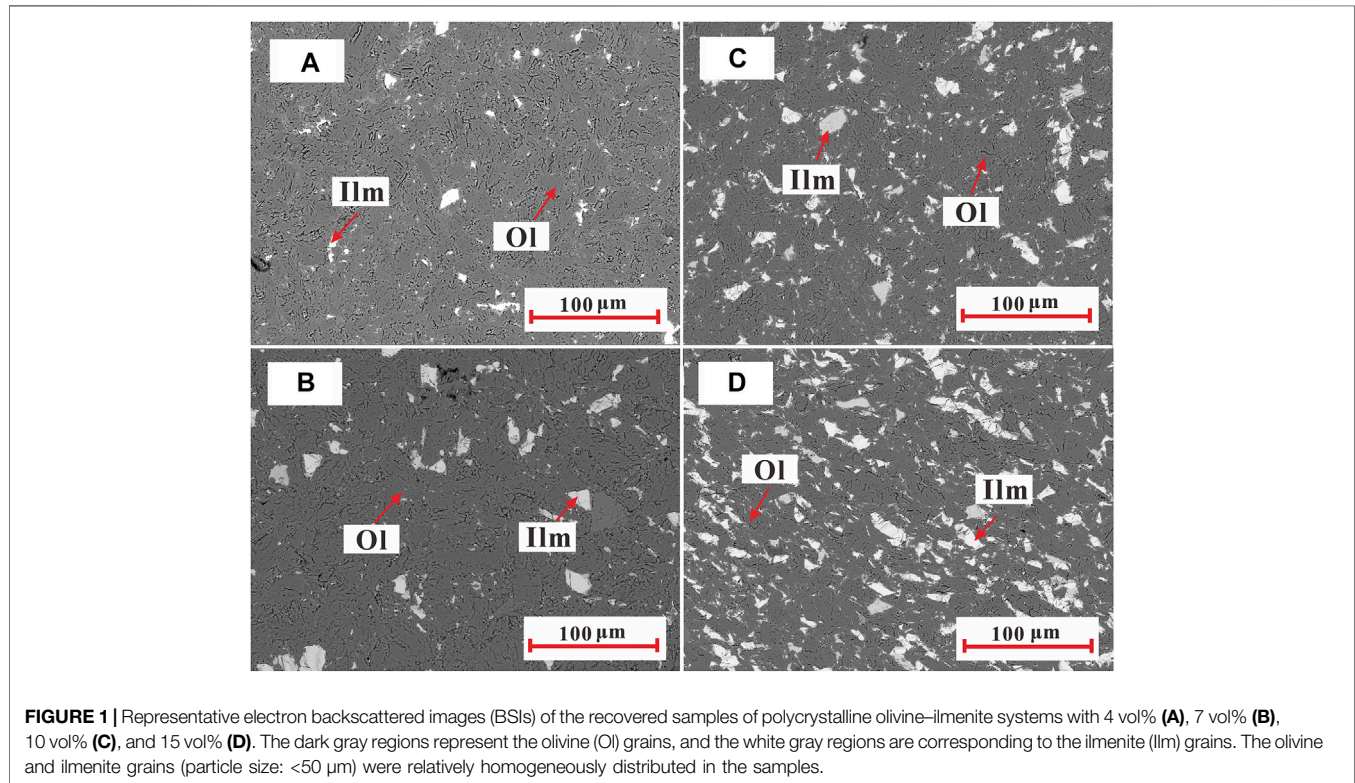
EXPERIMENTAL PROCEDURES

Sample Preparation

The main chemical compositions of the natural olivine and ilmenite grains were tested using the electron probe microanalysis, and the weight percentages of the oxides for the main elements were shown in **Table 1**. It is noted that the whole iron ions in the olivine and ilmenite were assumed to be ferrous iron, and the slight decrease of the total quantity of the oxides for ilmenite might be due to the presence of ferric irons and hematite (Andreozzi et al., 1996). Due to the very low decrease of the total quantity of oxides for ilmenite, it is revealed that the purity of ilmenite is very high. The fresh olivine and ilmenite grains were ultrasonically cleaned in a mixture of distilled water, acetone and ethanol, and ground to powder (<200 mesh) in an agate mortar. The olivine and ilmenite powders were homogeneously mixed by weight percent, and ilmenite contents of five powder samples were 5, 10, 13, 15, and 20 wt%, respectively. According to the weight fractions and densities of olivine (3.4 g/cm^3) and ilmenite (4.7 g/cm^3), the volume percent of ilmenite in the five olivine-ilmenite systems was 4, 7, 10, 11, and 15 vol%, respectively. The sample powder was loaded into a copper capsule with a 0.025-mm thick Ni-foil liner, and then sintered for 6 h in a multi-anvil high pressure apparatus at 2.0 GPa and 873 K. The hydrothermally annealed samples were cut and polished into cylinders with diameter and height of 6 mm, and ultrasonically cleaned in a mixture of deionized water, acetone and ethanol. In order to avoid the effect of absorbed water on the electrical conductivity measurements, all synthetic samples were dried at 423 K for 12 h in an oven. The mineral distribution and interior structure of the samples were observed by scanning electron microscopy at the State Key Laboratory of Ore Deposit Geochemistry, Institute of Geochemistry, Chinese Academy of Sciences (CAS), Guiyang, China. As shown in **Figure 1** the olivine and ilmenite grains were relatively uniformly distributed to the samples, and the particle-size ranges in various samples were close to each other. In order to determine the water content in the olivines, we applied the Fourier transform infrared (FTIR) spectrometer (Vertex-70 V

TABLE 1 | Chemical compositions of the initial olivine and ilmenite samples obtained using the electron probe microanalysis. The numbers represent the weight percent (wt.%) of the oxides for main elements of the olivine and ilmenite, and the whole iron elements are assumed to be ferrous irons.

Sample	FeO	MnO	NiO	Cr ₂ O ₃	Al ₂ O ₃	TiO ₂	SiO ₂	MgO	K ₂ O	CaO	Na ₂ O	V ₂ O ₃	CuO	Total
olivine	5.965	0.120	0.117	0.437	0.000	0.000	58.327	34.055	0.009	0.750	0.171	0.000	0.000	99.951
ilmenite	44.787	0.540	0.005	0.113	1.578	49.801	0.000	1.562	0.000	0.000	0.000	0.262	0.008	98.656



and Hyperion-1000 infrared microscope) in the Key Laboratory of High-temperature and High-pressure Study of the Earth's Interior, Institute of Geochemistry, Chinese Academy of Sciences, China. The infrared spectra were measured with unpolarized radiation from a mid-IR light source, a mercury-cadmium-telluride detector (aperture size: 100 × 100 μm) and a CaF₂ beam splitter. The FTIR spectra in wavenumber range of 3,000–4,000 cm⁻¹ with 512 scans of the original and annealed olivine grains were obtained. After simple base and smooth treatments, the infrared spectra of the original and annealed olivines were almost flat (Figure 2), indicating no water was absorbed in the original and annealed olivines.

Impedance Measurements

Electrical conductivity measurements were performed in the YJ-3000t multi-anvil apparatus and Solartron-1260 impedance/gain-phase analyzer at the Key Laboratory of High-Temperature and High-Pressure Study of the Earth's Interior, Institute of Geochemistry, CAS, Guiyang, China. The large-volume high-pressure press and complex impedance analyzer have been widely

applied to study the electrical conductivities of a series of minerals and rocks (Wang et al., 2010; Dai et al., 2015a; Dai et al., 2015b, Dai et al., 2016, Dai et al., 2018; Hu et al., 2014, Hu et al., 2017, Hu et al., 2018; Sun et al., 2017). During operation of the high-pressure press, six cubic WC anvils (side length: 25 mm) were driven by oil pressure to compress the cubic sample assembly, providing the pressures of up to 3.0 GPa. Using the lanthanum chromate and stainless steel as heater, temperatures of up to 2,273 and 1573 K can be achieved, respectively. The schematic diagram of the sample assembly for electrical conductivity measurements was shown in Figure 3. In order to remove the water in the sample assembly, all relevant components were baked in a 1073 K muffle furnace for 6 h. A pyrophyllite cube (32.5 × 32.5 × 32.5 mm³) and stainless-steel sheets (thickness: 0.5 mm) were used as the pressure medium and heater, respectively. Alumina and magnesia sleeves were located adjacent to the heater as insulators and pressure medium. To shield against external electromagnetism and spurious signal interference, a layer of nickel foil was placed between the Al₂O₃ and MgO sleeves. The MgO tube (inner diameter: 6 mm, height: 20 mm) was applied as

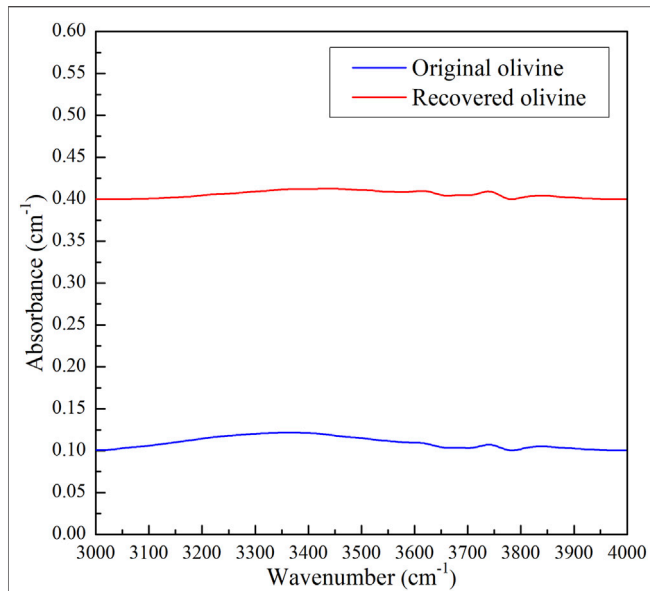


FIGURE 2 | Fourier transform infrared (FTIR) spectra of the original and recovered olivines in the wavenumbers range of 3,000–4,000 cm^{-1} .

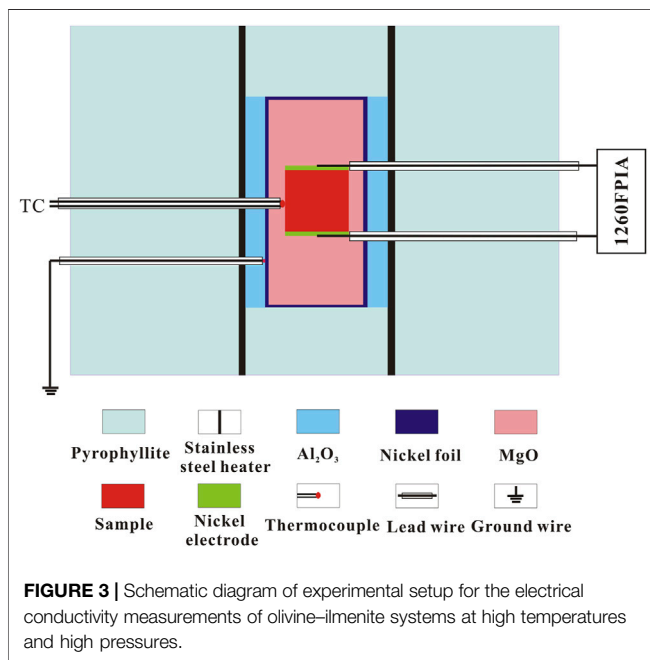


FIGURE 3 | Schematic diagram of experimental setup for the electrical conductivity measurements of olivine-ilmenite systems at high temperatures and high pressures.

sample capsule. The parallel-plate electrode was composed of two nickel disks with the diameter of 6.0 mm and thickness of 0.5 mm. In addition, the nickel electrode and nickel foil can be used to control the oxygen fugacity in the sample capsule at high temperatures and high pressures. It has been demonstrated that the oxygen fugacity controlled by Ni-NiO buffer (NNO) at high temperature and high pressure is close to the oxygen fugacity of the Earth's upper mantle (Xu et al., 2000; Dai et al., 2012). And then, the K-type thermocouple wires (NiCr/NiSi) and ground

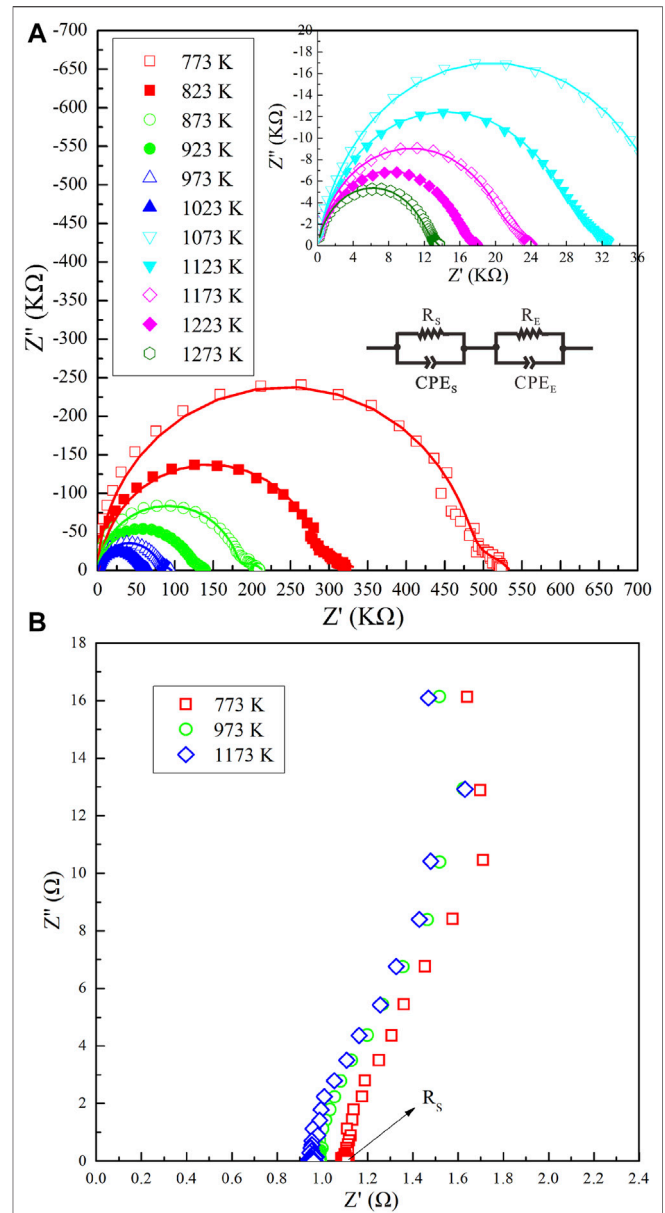


FIGURE 4 | Typical complex impedance spectra for (A) polycrystalline olivine-ilmenite system with 10 vol% ilmenites and (B) pure ilmenite aggregates under the conditions of 2 GPa and various temperatures.

wire (NiSi) were inserted into the holes in the lateral edge of the pyrophyllite cube, and contacted with the sample and nickel foil, respectively. To keep dry, the sample assembly was placed in a 323 K oven for at least 12 h before electrical conductivity measurements.

During the experiments, the pressure was slowly raised at a rate of 0.5 GPa/h until it reached the desired value, and then the temperature was increased with a speed of 10 K/min to the designated value. Under the stable pressure and temperature, impedance spectra of the samples were collected in the frequency range of 10^{-1} – 10^6 Hz at the constant exciting voltage of 1,000 mV. The measurement temperatures change with a 50-K

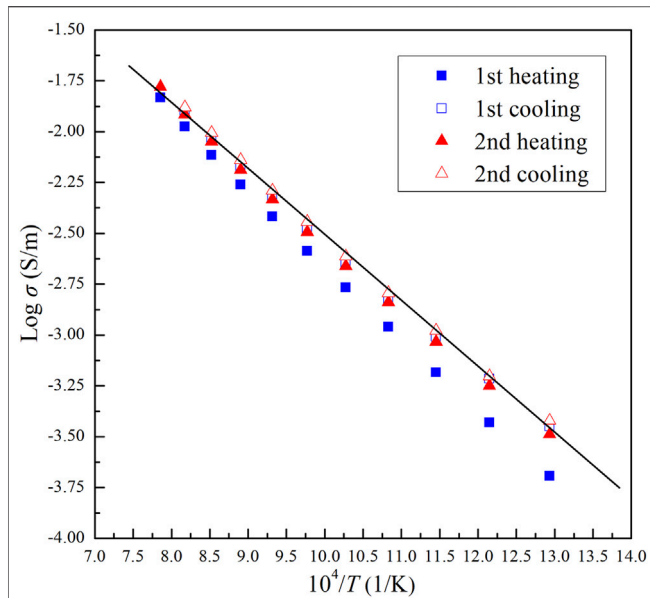


FIGURE 5 | Logarithmic electrical conductivity versus reciprocal temperature for dry olivine aggregates with 10 vol% chromite during multiple heating/cooling cycles at 2.0 GPa and 773–1273 K.

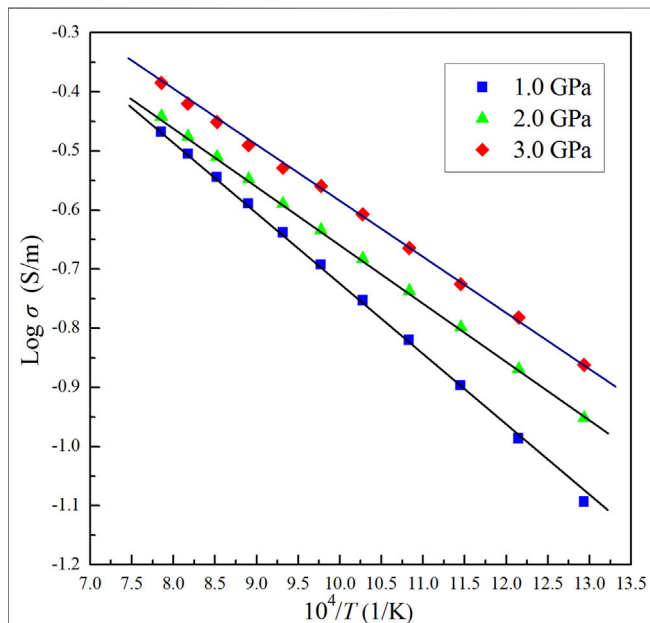


FIGURE 6 | The linear relationship between Logarithmic electrical conductivities and reciprocal temperatures for olivine-ilmenite system with 11 vol% ilmenites under the conditions of 1.0–3.0 GPa and 773–1273 K.

interval. To obtain reproducible data, impedance spectra of samples were collected in multiple heating/cooling cycles under conditions of 1.0–3.0 GPa and 773–1273 K. The errors of temperature and pressure were ± 5 K and ± 0.1 GPa, respectively.

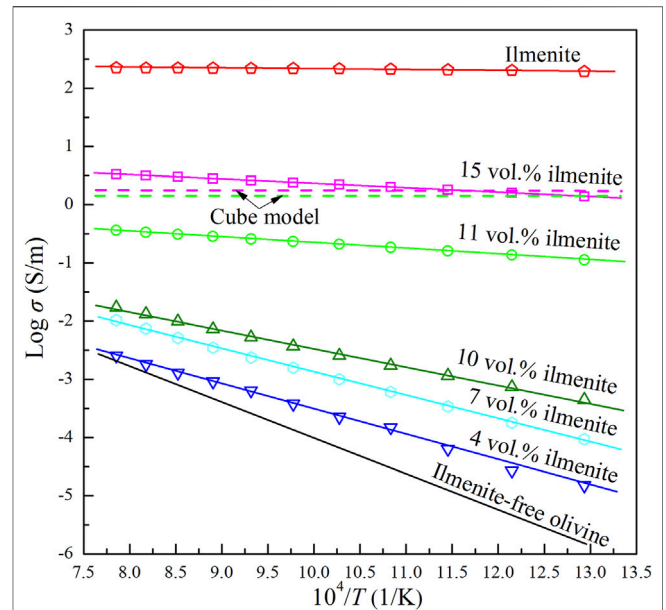


FIGURE 7 | Logarithm of electrical conductivities versus reciprocal temperatures for pure olivine aggregates, polycrystalline olivine with various ilmenite contents (4–15 vol%), and pure ilmenite aggregates at 2.0 GPa and 873–1273 K. The solid lines represent the measurement conductivities of pure olivine aggregates (Dai et al., 2019), olivine-ilmenite systems and pure ilmenite aggregates, and green and pink dash lines stand for the calculated conductivities of olivine-ilmenite systems with 11 vol% and 15 vol% using cube model, respectively.

RESULTS

Representative complex impedance spectra of the dry olivine-ilmenite systems and pure ilmenite aggregates were shown in **Figure 4**. For the pure ilmenite aggregates, the impedance spectra were approximate perpendicular lines, and the intercepts of the lines in the horizontal axis represented the electrical resistances. For the olivine-ilmenite systems, the impedance spectra were composed of an almost ideal semicircle in the high-frequency region and an additional tail in the low-frequency region. Previous studies have proposed that the ideal semicircle in the high-frequency region represents the bulk electrical properties of the sample, and the additional tail is related to the diffusion processes at the sample-electrode interface (Roberts and Tyburczy, 1991; Dai and Karato, 2009; Yang et al., 2012). Therefore, the bulk sample resistance can be obtained by fitting the ideal semicircle in the high-frequency region. A series connection of R_S - CPE_S (R_S and CPE_S represent the resistance and constant-phase element of the sample, respectively) and R_E - CPE_E (R_E and CPE_E represent the resistance and constant-phase element for electrode effect, respectively) were used as the equivalent circuit, and the fitting errors of the electrical resistance were less than 5%. The electrical conductivities of the olivine-ilmenite systems were calculated using the following formula:

$$\sigma = L/SR \quad (1)$$

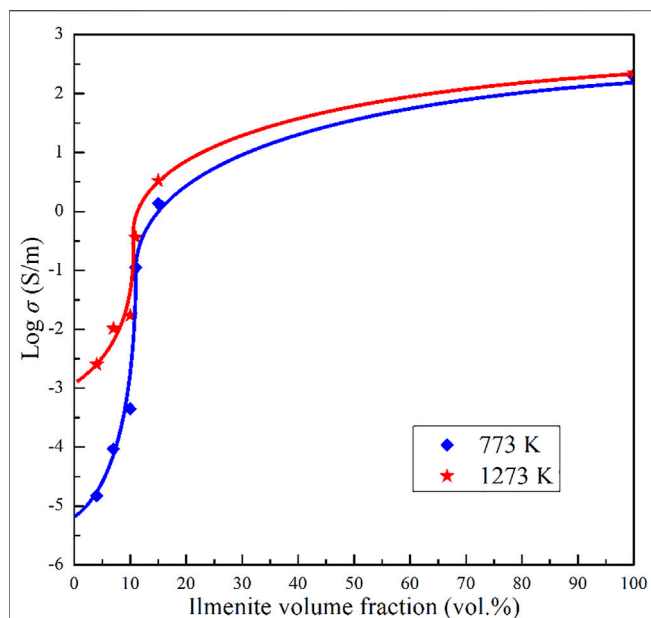


FIGURE 8 | The relationships between logarithmic conductivities of the olivine–ilmenite systems and ilmenite volume fractions at 773 and 1273 K. The diamond symbols and five-star symbols stand for the measured values of electrical conductivities, and solid lines represented the fitted curves.

where L is the height of the sample (m), S is the cross-sectional area of the electrodes (m^2), R is the fitting resistance (Ω), and σ is the electrical conductivity of the sample (S/m).

The impedance spectra of the olivine–ilmenite systems were collected in multiple heating/cooling cycles, and the final stable data were applied to discuss the relevant laws. As shown in **Figure 5**, the electrical conductivities of olivine–ilmenite system with 10 vol% ilmenite were almost repeated in the 2nd heating/cooling cycles. In order to investigate the relationship between the conductivities and temperatures and pressures, we plotted the logarithmic conductivities versus temperatures at the constant pressures. The reproducible data were applied to analyze the electrical properties of the samples at high temperatures and pressures. **Figure 6** revealed pressure influence on the conductivities of the olivine aggregates mixed with 11 vol% ilmenites under the conditions of 1.0–3.0 GPa and 773–1273 K. Pressure was positively related to the conductivities of olivine–ilmenite systems, being the opposite influence for pure olivine aggregates (Dai et al., 2010; Dai et al., 2019). Influence of pressure on the conductivities of the olivine–ilmenite systems was much weaker than that of temperature (**Figure 6**), further supporting the previous conclusion for the slight influence of pressure on the conductivities of silicate minerals with or without some other high-conductivity minerals (Wang et al., 2010; Yang et al., 2011; Hu et al., 2014; Dai et al., 2019; Guo et al., 2020). **Figure 7** showed the influence of ilmenite contents on the conductivities of olivine–ilmenite systems at 2.0 GPa and 773–1273 K. Electrical conductivities of olivine–ilmenite systems with the ilmenite volume fractions of 0–10 vol% moderately increased with increasing ilmenite content. The conductivities of

olivine–ilmenite system with 10 vol% ilmenites were about 0.5 orders of magnitude higher than those of the system with 7 vol% ilmenites. However, the conductivities of olivine aggregates with 11 vol% ilmenites were ~ 1.5 –3 orders of magnitude higher than those for olivine–ilmenite system with 10 vol% ilmenites. And then, the conductivities of olivine–ilmenite system with 15 vol% ilmenites were about 1 order of magnitude higher than those of the system with 11 vol% ilmenites (**Figure 7**). It was clear that the conductivities of olivine–ilmenite systems dramatically increased at the ilmenite content of 11 vol% (**Figure 8**). And thus, the ilmenite grains in the olivine–ilmenite system with 11 vol% ilmenites might be interconnected. In order to further verify the above inference, we applied Cube model which was suitable for the systems with interconnected high-conductivity phase to calculate the conductivities of olivine–ilmenite systems with 11 vol% and 15 vol% ilmenites. The mathematical formula for the cube model is expressed as:

$$\sigma_b = (1 - (1 - \Phi)^{\frac{3}{2}})\sigma_i \quad (2)$$

where σ_b and σ_i are the conductivities of the olivine–ilmenite system and ilmenite aggregates, respectively, Φ is the ilmenite content. Unexpectedly, for the conductivities of olivine–ilmenite systems with 11 vol% ilmenites, the measurement values was 0.5–1.0 orders lower than the calculated values using Cube model; for the conductivities of olivine–ilmenite systems with 15 vol% ilmenites, the measurement values was very close to the calculated values from Cube model (**Figure 7**). It was proposed that ilmenite grains in the olivine–15 vol% ilmenite system were well interconnected, but locally interconnected in olivine–11 vol% ilmenite system. According to the linear relations between the logarithmic conductivities of the olivine–ilmenite systems and reciprocal temperatures (**Figure 7**), the conductivities and temperatures at a certain pressure conformed to the Arrhenius formula,

$$\sigma = \sigma_0 \exp(-\Delta H/kT) \quad (3)$$

where σ_0 is the pre-exponential factor (KS/m), k is the Boltzmann constant (eV/K), T is the absolute temperature (K), and ΔH is the activation enthalpy (eV). The relevant fitting thermodynamic parameters for electrical conductivities of the samples were listed in **Table 2**. Activation enthalpies of the charge carriers for the pure ilmenite aggregates, olivine–ilmenite systems with interconnected and isolated ilmenites were 0.01, 0.15–0.24, 0.62–0.89 eV, respectively, being much lower than the enthalpy for olivine aggregates (1.27 eV) from Dai et al. (2019). The activation enthalpies for the olivine–ilmenite systems dramatically decreased at the ilmenite content of 11 vol% (**Figure 9**), corresponding to the significant increase of the electrical conductivities (**Figure 8**).

DISCUSSIONS

Comparisons With Previous Studies

Under the conditions of 2.0 GPa and 773–1273 K, electrical conductivities of the pure olivine aggregates (Dai et al., 2019),

TABLE 2 | Fitted parameters for the Arrhenius relations for the electrical conductivities of the dry olivine aggregates with various volume percents of ilmenite (V_{ilm}).

Sample	V_{ilm} (Vol%)	P (GPa)	T (K)	$\text{Log } \sigma_0$ (S/m)	ΔH (eV)	R^2
Olivine (Ol) ^a	0	2.0	773–1,273	1.27 ± 0.03	1.27 ± 0.01	99.76
Ol-Ilm system ^b	4	2.0	773–1,273	0.93 ± 0.08	0.89 ± 0.02	99.68
Ol-Ilm system ^b	7	2.0	773–1,273	1.14 ± 0.04	0.80 ± 0.01	99.92
Ol-Ilm system ^b	10	2.0	773–1,273	0.65 ± 0.05	0.62 ± 0.01	99.71
Ol-Ilm system ^b	11	1.0	773–1,273	0.50 ± 0.01	0.24 ± 0.01	99.93
Ol-Ilm system ^b	11	2.0	773–1,273	0.34 ± 0.01	0.20 ± 0.01	99.98
Ol-Ilm system ^b	11	3.0	773–1,273	0.34 ± 0.01	0.18 ± 0.01	99.96
Ol-Ilm system ^b	15	2.0	773–1,273	1.12 ± 0.01	0.15 ± 0.01	99.97
Ilmenite (Ilm) ^p	100	2.0	773–1,273	2.44 ± 0.01	0.01 ± 0.00	90.83

Note: *a* and *b* stand for the experimental samples from Dai et al. (2019) and the present study, respectively.

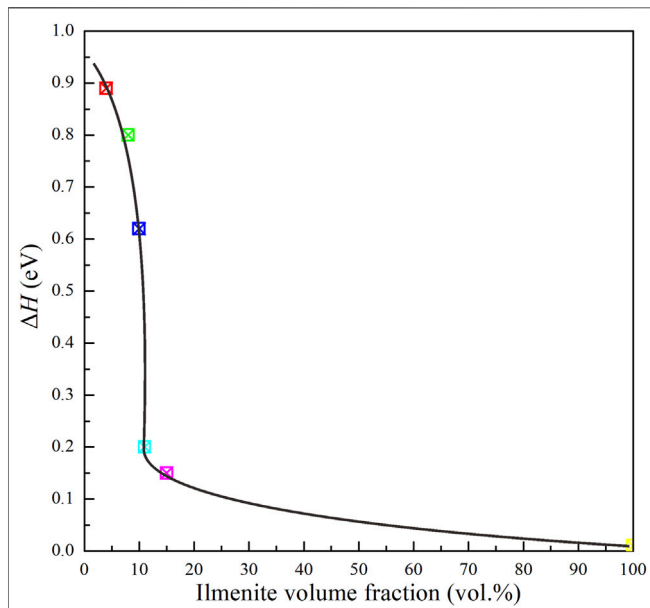


FIGURE 9 | Activation enthalpies of charge carriers for olivine–ilmenite systems versus the volume fractions of ilmenites at 2.0 GPa and 773–1273 K.

olivine–ilmenite systems with isolated ilmenites, olivine–ilmenite systems with interconnected ilmenites and pure ilmenite aggregates were about 10^{-5} – 10^{-3} , 10^{-5} – 10^{-2} , 10^{-1} – $10^{-0.5}$ and $10^{2.5}$ S/m, respectively. It was indicated that the conductivities of the olivine–ilmenite systems increased with increasing content of ilmenite. According to the abrupt changes of the conductivities and activation enthalpies for the olivine–ilmenite systems, the percolation threshold of the ilmenite grains in the olivine aggregates was proposed to be about 11 vol%. Effect of temperature on the conductivities of the olivine aggregates and olivine–ilmenite systems with isolated ilmenite were much greater than those of the olivine–interconnected ilmenite systems. It might be due to the activation enthalpies for olivine–ilmenite systems decreased with increasing ilmenite contents. Some previous studies have researched the electrical conductivities of olivine aggregates with other high-conductivity mineral phases at high temperatures and high pressures

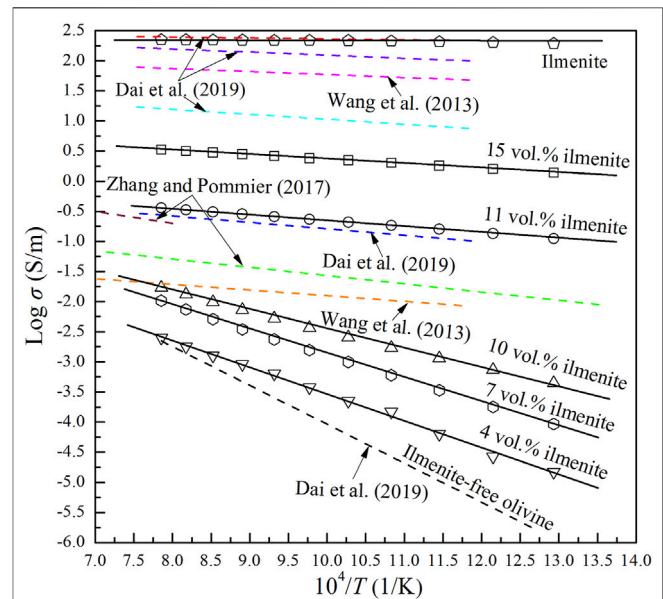


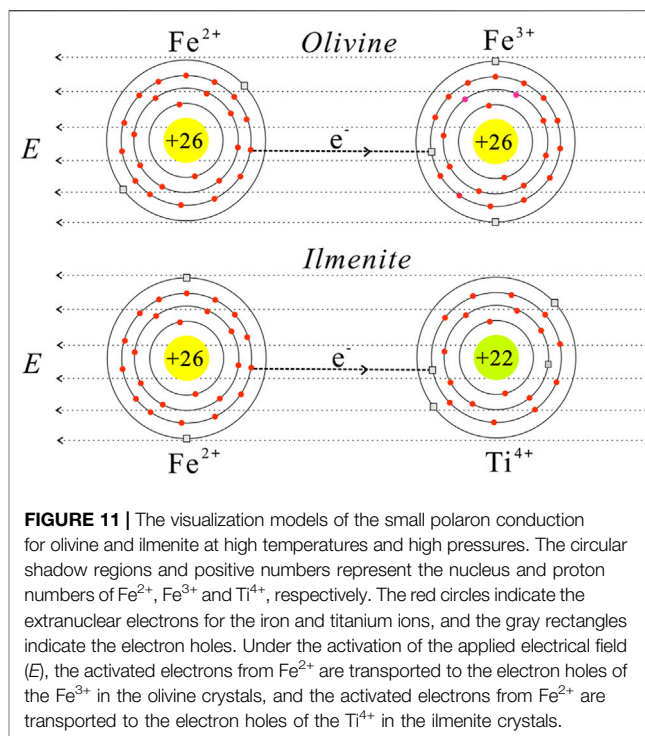
FIGURE 10 | Electrical conductivities of olivine–ilmenite systems with various ilmenite contents compared with other relevant olivine systems at high temperatures and high pressures. The solid black lines with various symbols denoted the conductivities of olivine–ilmenite systems with various ilmenite contents in this study, the dashed orange and pink lines stood for the conductivities of olivine–magnesian–diamond and olivine graphite systems (7 vol% graphite) at 4.0 GPa, respectively (Wang et al., 2013); the dashed green and brown lines indicated the results of the olivine–FeS systems with 10 vol% and 12 vol% FeS at 4.7–6.1 GPa, respectively (Zhang and Pommier, 2017); the dashed black, sky blue, pink, purple and red lines represented the conductivities of pure olivine aggregates, olivine–3 vol% magnetite system, olivine–10 vol% magnetite system, olivine–20 vol% magnetite system and pure ilmenite aggregates at 2.0 GPa, respectively (Dai et al., 2019).

(Figure 10). Graphite is widely distributed in cratonic lithospheric mantle (Pearson et al., 1994), and thus plays a significant role on the electrical structure of the stable regions of upper mantle. Wang et al. (2013) researched the conductivities of olivine aggregates with various contents of graphite at 4 GPa and 1,173–1,673 K. When the concentration of graphite exceeds percolation threshold (~ 1 wt%), the conductivities of olivine aggregates with graphite was markedly enhanced. Zhang and Pommier (2017) investigated the conductivities of metal–olivine

systems at ~ 5–6 GPa and up to 1948 K. Both the metal: olivine ratio and the metal phase geometry influenced the electrical conductivities of the two-layer samples. Dai et al. (2019) studied the electrical conductivities of olivine with various contents of magnetite under the conditions of 2.0 GPa and 873–1273 K. The conductivities of olivine–magnetite systems dramatically increased with increasing magnetite contents, and the percolation threshold of magnetite in the olivine aggregates was about 3 vol%. As shown in **Figure 10**, the conductivities of olivine–11 vol% ilmenite system were very close to those of olivine–3 vol% magnetite and olivine–12 vol% FeS systems, but 3–6 orders of magnitude higher than those of the olivine aggregates; the conductivities of olivine–10 vol% ilmenite system were much lower than those of olivine–4 vol% graphite system at lower-temperature range, but close to each other at higher temperature range. The conductivities of olivine–10 vol% FeS system were slightly higher than those of olivine–4 vol% graphite system. In addition, the conductivities of olivine–15 vol% ilmenite system were about 0.75 orders of magnitude lower than those of the olivine–10 vol% magnetite system, whose conductivities were about 1 order of magnitude lower than those of olivine–7 vol% graphite system. Furthermore, the conductivities of ilmenite aggregates were very close to those of magnetite aggregates, slightly higher than those of olivine–20 vol% magnetite system, and 2 orders of magnitude higher than those of olivine–15 vol% ilmenite system. According to the above analysis, we proposed that the graphite and magnetite grains were more easily interconnected than ilmenite grains in the olivine aggregates. The percolation thresholds of various high-conductivity minerals in the olivine aggregates are possibly dominated to the particle sizes, plasticity and interface energy of the high-conductivity minerals.

Conduction Mechanism

The logarithmic electrical conductivities of the dry olivine–ilmenite systems and reciprocal temperatures conformed to only one linear relationship under the experimental conditions (**Figure 7**). This was revealed that the conductivities of a certain olivine–ilmenite system were chiefly constrained by one major conduction mechanism at 1.0–3.0 GPa and 773–1273 K. According to the previous studies, small polaron, proton, and alkali ions were proposed to be the significant charge carriers for silicate minerals and rocks (Wang et al., 2006; Dai et al., 2010; Dai et al., 2018; Karato, 2013; Hu et al., 2014; Hu et al., 2018; Guo et al., 2020). In addition, the main conduction mechanism for a certain mineral was changed with the variation of chemical compositions. The electrical conductivities and conduction mechanisms for natural and synthetic olivine with various chemical compositions have been widely researched, and small polaron and proton conduction was proposed to be the dominant conduction mechanism for the anhydrous and hydrous olivine, respectively. (e.g., Wang et al., 2006; Poe et al., 2010; Karato, 2013; Dai and Karato, 2014; Dai et al., 2019). There was no obvious absorption peak being observed in the FT-IR spectra of the original and recovered olivine (**Figure 2**). And thus, proton conduction was excluded from the possible conduction



mechanism for the olivine. The small polaron conduction was proposed to be the conduction mechanism for dry olivine, reference to Dai et al. (2019). For the ilmenite (FeTiO_3), the activation enthalpy (0.01 eV) was much lower than those for the ionic conduction (Hu et al., 2014), proton conduction (Dai and Karato, 2014) and small polaron conduction (Zhang et al., 2017). The crystal structure of ilmenite was same with that of geikielite (MgTiO_3), and the activation enthalpy for iron-bearing ilmenite (0.01 eV) was much lower than the values (0.23–0.39 eV) for geikielite (Parthasarathy, 2011). The discrepancy might be due to the presence of iron in the ilmenite. Parthasarathy (2011) proposed that the conduction mechanism of geikielite is closely related to the electron transport. In contrast to geikielite, ferrous ions occupy the lattice positions of the ilmenite. Both iron and titanium ions in the ilmenite crystal are variable valence elements, and thus the conduction mechanism for pure ilmenite is proposed to be the small polaron conduction. The conduction processes of the small polarons in the olivine and ilmenite were displayed in **Figure 11**. Electrical conductivity of a mineral or rock was the result of directed migration of all charge carrier species, and the corresponding expression was displayed as follow:

$$\sigma = \sum_j q_j n_j \mu_j \quad (4)$$

where q_j , n_j and μ_j are the effective charge, quantity and mobility of the j -type charge carrier in the sample. Electrical conductivity of ilmenite was much higher than that of olivine (**Figure 7**), indicating the quantity and mobility of small polarons in the ilmenite crystals were superior to those in the olivine crystals. As a

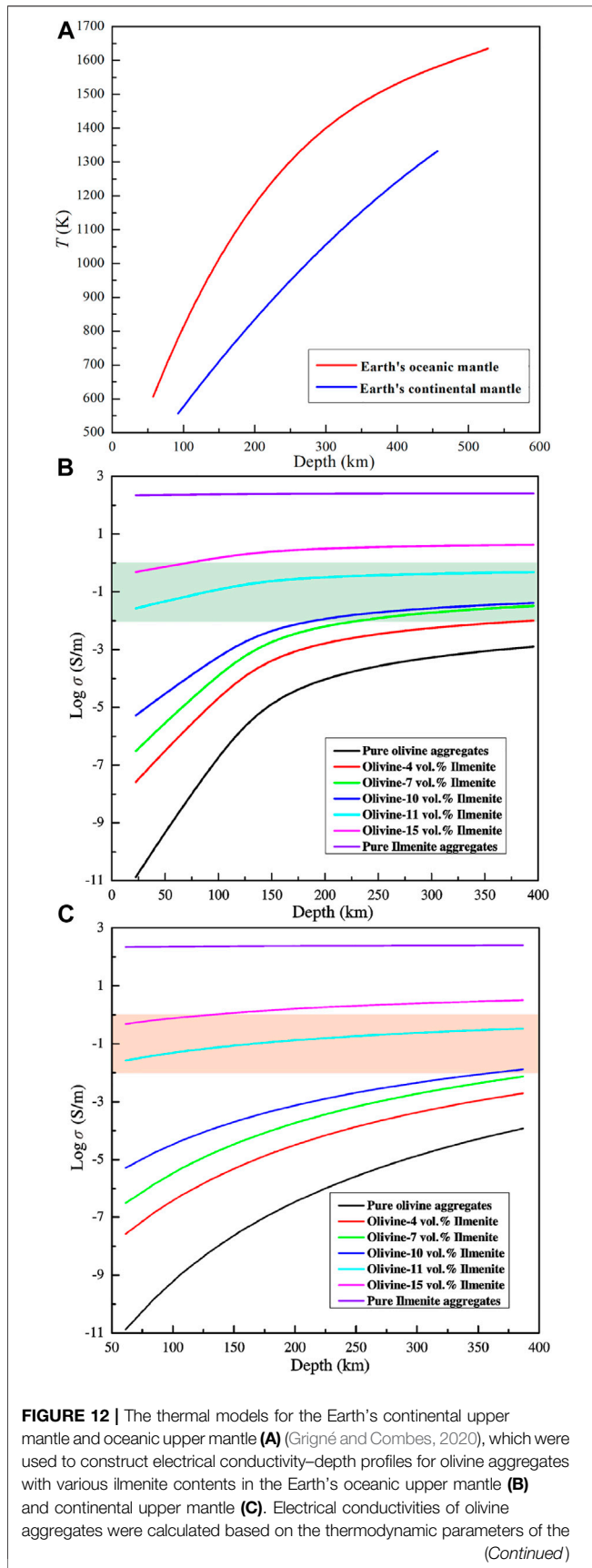


FIGURE 12 | Arrhenius relation (Dai et al., 2019), and the conductivities of the olivine–ilmenite systems and ilmenite aggregates were calculated based on the thermodynamic parameters in this study. The solid lines presented the electrical conductivity–depth profiles of the olivine–ilmenite systems, and shadow regions indicated the high conductivity anomalies in the Earth's oceanic upper mantle and continental upper mantle.

consequence, the conductivities of olivine–ilmenite systems increased with the increase of ilmenite content. The activation enthalpies of the olivine–ilmenite systems with isolated ilmenites (0.62–0.89 eV) were much higher than those for the samples with interconnected ilmenites (0.15–0.20 eV). This revealed that the ilmenite mainly constrained the electrical conductivities of the dry olivine aggregates with interconnected ilmenites, and the dominant charge carriers are the small polarons in the ilmenite crystals. According to the previous studies, the electrical conductivities of the minerals and rocks with the small polaron conduction increase with the increase of oxygen fugacity at high temperatures and high pressures (Dai et al., 2008; Dai et al., 2012). It was implied that the electrical conductivities of the olivine–ilmenite systems probably increase with the increase of oxygen fugacity to some extent. The oxygen fugacity controlled by NNO buffer is close to the oxygen fugacity of the normal region in the Earth's upper mantle (Xu et al., 2000; Dai et al., 2012), and our measured electrical conductivity only represents the conductivity of the peridotite with a certain amount of ilmenite in the regions where the oxygen fugacity is close to that controlled by NNO buffer.

Geophysical Implications

Ilmenite exists as the inclusion in olivine and the accessory mineral of mantle derived mafic rock (Hacker et al., 1997; Risold et al., 2003; Carter Hearn Jr, 2004; Litasov et al., 2003; Bali et al., 2018). The estimated contents of ilmenite in some mafic rocks were lower than 10 vol% based on the scanning electronic microscope images of the natural samples (Risold et al., 2003; Litasov et al., 2003). In some special regions, ilmenite deposits were formed by the magmatism which closely related to the mantle plume (Xu et al., 2001; Charlier et al., 2010). In Emeishan Large Igneous Province (ELIP), ilmenites were enriched in the ultra-basic rocks formed in the process of mantle plume activity in the late Permian (Zhang et al., 2008; Zhang et al., 2009; She et al., 2015). This implied that ilmenite components in the upper mantle might be converged in the magmatism. The conductivities of the olivine aggregates with various ilmenite contents can be applied to invert the magnetotelluric (MT) profiles, and further research electrical structures of the Earth's upper mantle. Combining with the electrical conductivities of olivine–ilmenite systems and the thermal models of the Earth's continental upper mantle and oceanic upper mantle (Grigné and Combes, 2020), the electrical conductivity–depth profiles of the olivine aggregates with various ilmenite contents in the continental and oceanic upper mantles were constructed in detail (Figures 12A–C). As shown in Figure 12, the conductivities of dry olivine aggregates with a certain content of ilmenites at the same depth beneath the

continental plate and oceanic plate were different due to the various thermodynamic conditions. In addition, the electrical conductivity of a certain olivine-ilmenite system increased with depth due to the increase of temperature. According to the MT profiles, the range of the anomaly high electrical conductivity in the upper mantle is about 10^{-2} – 10^0 S/m (Dong et al., 2014; Adetunji et al., 2015). Electrical conductivities of dry olivine aggregates with 11–15 vol% ilmenite (10^{-1} – $10^{0.5}$ S/m) were close to those of the high conductivity layers (10^{-2} –1 S/m) in the upper mantle (Figure 12). It was implied that the presence of interconnected ilmenite can interpret the high conductivity anomalies in the upper mantle. However, the ilmenite contents in the natural peridotites are much lower than the threshold percolation (11 vol%) for ilmenite, and it is not clear whether ilmenite can reach interconnected state in the present upper mantle. We proposed that the interpretation of high conductivity anomalies using the interconnected ilmenites should be cautious unless the interconnected ilmenites are demonstrated to exist in the upper mantle in the future.

CONCLUSIONS

Electrical conductivities of dry olivine-ilmenite systems with various contents of ilmenite ($V_{\text{ilm}} = 4, 7, 10, 11, 15$ vol%) and pure ilmenite aggregates were $\sim 10^{-5}$ – $10^{0.5}$ and $\sim 10^{2.5}$ S/m, respectively, under the conditions of 1.0–3.0 GPa and 773–1273 K. Temperature moderately enhanced the conductivities of olivine-ilmenite systems, but the positive effect of pressure was slight. Based on the inflection point for the relationship between electrical conductivities of the systems and ilmenite contents, we proposed that the percolation threshold of the ilmenite grains in the dry olivine-ilmenite systems was about 11 vol%. Interconnected ilmenites dramatically enhanced the conductivities of the olivine-ilmenite systems. In addition, activation enthalpies for the charge carriers of olivine-ilmenite systems (0.15–0.89 eV) decreased with increasing ilmenite

contents. The dominant conduction mechanism for the whole olivine-ilmenite systems is small polaron conduction. Electrical conductivity-depth profiles of olivine-ilmenite systems in the Earth's upper mantle have been constructed, being beneficial to research the electrical structures in the Earth's interior. Ilmenite can play an important role on the electrical properties of some special regions in the Earth's interior. Due to the percolation threshold (11 vol%) for the interconnectivity of ilmenites is much higher than the volume percentages of ilmenites in the natural peridotites, it should be very cautious to interpret the high conductivity anomalies in the Earth's upper mantle (Dai and Karato, 2020).

DATA AVAILABILITY STATEMENT

The original contributions presented in the study are included in the article/Supplementary Material, further inquiries can be directed to the corresponding authors.

AUTHOR CONTRIBUTIONS

LD and HH (designing the project). WS and MW (conducting high-P experiments). WS (writing the initial draft of the work). LD, HH, WS, MW, ZH, and CJ (interpreting the results).

FUNDING

This research was financially supported by the NSF of China (42072055, 41774099, 41772042 and 42002043), Youth Innovation Promotion Association of CAS (Grant No. 2019390), Special Fund of the West Light Foundation of CAS, and as well as the Science and Technology Foundation of Guizhou Province (QKHJZ (2013) 2285).

REFERENCES

- Adetunji, A. Q., Ferguson, I. J., and Jones, A. G. (2015). Reexamination of Magnetotelluric Responses and Electrical Anisotropy of the Lithospheric Mantle in the Grenville Province, Canada. *J. Geophys. Res. Solid Earth* 120, 1890–1908. doi:10.1002/2014JB011713
- Andreozzi, G. B., Cellucci, F., and Gozzi, D. (1996). High-temperature Electrical Conductivity of FeTiO₃ and Ilmenite. *J. Mater. Chem.* 6, 987–991. doi:10.1039/jm9960600987
- Bali, E., Hidas, K., Guðfinnsson, G. H., Kovács, Z., Török, K., and Román-Alpiste, M. J. (2018). Zircon and Apatite-Bearing Pyroxene Hornblende Mantle Xenolith from Hungary, Carpathian-Pannonian Region. *Lithos* 316–317, 19–32. doi:10.1016/j.lithos.2018.07.004
- Cao, Y., Wang, C. Y., Huang, F., and Zhang, Z. (2019). Iron Isotope Systematics of the Panzhihua Mafic Layered Intrusion Associated with Giant Fe-Ti Oxide Deposit in the Emeishan Large Igneous Province, SW China. *J. Geophys. Res. Solid Earth* 124, 358–375. doi:10.1029/2018jb016466
- Carter Hearn Jr., B. (2004). The Homestead Kimberlite, central Montana, USA: Mineralogy, Xenocrysts, and Upper-Mantle Xenoliths☆. *Lithos* 77, 473–491. doi:10.1016/j.lithos.2004.04.030
- Charlier, B., Namur, O., Malpas, S., de Marneffe, C., Duchesne, J.-C., Auwera, J. V., et al. (2010). Origin of the Giant Allard Lake Ilmenite Ore deposit (Canada) by Fractional Crystallization, Multiple Magma Pulses and Mixing. *Lithos* 117, 119–134. doi:10.1016/j.lithos.2010.02.009
- Dai, L., Li, H., Li, C., Hu, H., and Shan, S. (2010). The Electrical Conductivity of Dry Polycrystalline Olivine Compacts at High Temperatures and Pressures. *Mineral. Mag.* 74, 849–857. doi:10.1180/minmag.2010.074.5.849
- Dai, L., Li, H., Hu, H., Shan, S., Jiang, J., and Hui, K. (2012). The Effect of Chemical Composition and Oxygen Fugacity on the Electrical Conductivity of Dry and Hydrated Garnet at High Temperatures and Pressures. *Contrib. Mineral. Petrol.* 163, 689–700. doi:10.1007/s00410-011-0693-5
- Dai, L., Jiang, J., Li, H., Hu, H., and Hui, K. (2015a). Electrical Conductivity of Hydrated Natural Basalts at High Temperatures and Pressures. *J. Appl. Geophys.* 112, 290–297. doi:10.1016/j.jappgeo.2014.12.007
- Dai, L., Hu, H., Li, H., Hui, K., Jiang, J., Li, J., et al. (2015b). Electrical Conductivity of Gabbro: the Effects of Temperature, Pressure and Oxygen Fugacity. *Eur. J. Mineralogy* 27, 215–224. doi:10.1127/ejm/2015/0027-2429
- Dai, L. D., Hu, H. Y., Li, H. P., Wu, L., Hui, K. S., Jiang, J. J., et al. (2016). Influence of Temperature, Pressure, and Oxygen Fugacity on the Electrical Conductivity of Dry Eclogite, and Geophysical Implications. *Geochem. Geophys. Geosyst.* 17, 2394–2407. doi:10.1002/2016gc006282

- Dai, L. D., Li, H. P., Hu, H. Y., and Shan, S. M. (2008). Experimental Study of Grain Boundary Electrical Conductivities of Dry Synthetic Peridotite under High-temperature, High-pressure, and Different Oxygen Fugacity Conditions. *J. Geophys. Res. Solid Earth* 113, B12211. doi:10.1029/2008JB005820
- Dai, L. D., Sun, W. Q., Li, H. P., Hu, H. Y., Wu, L., and Jiang, J. J. (2018). Effect of Chemical Composition on the Electrical Conductivity of Gneiss at High Temperatures and Pressures. *Solid Earth* 9, 233–245. doi:10.5194/se-9-233-2018
- Dai, L., Hu, H., Sun, W., Li, H., Liu, C., and Wang, M. (2019). Influence of High Conductive Magnetite Impurity on the Electrical Conductivity of Dry Olivine Aggregates at High Temperature and High Pressure. *Minerals* 9, 44. doi:10.3390/min9010044
- Dai, L., and Karato, S.-i. (2009). Electrical Conductivity of Pyrope-Rich Garnet at High Temperature and High Pressure. *Phys. Earth Planet. Interiors* 176, 83–88. doi:10.1016/j.pepi.2009.04.002
- Dai, L., and Karato, S.-i. (2014). Influence of FeO and H on the Electrical Conductivity of Olivine. *Phys. Earth Planet. Interiors* 237, 73–79. doi:10.1016/j.pepi.2014.10.006
- Dai, L., and Karato, S.-i. (2020). Electrical Conductivity of Ti-bearing Hydrous Olivine Aggregates at High Temperature and High Pressure. *J. Geophys. Res. Solid Earth* 125, e2020JB020309. doi:10.1029/2020JB020309
- Dong, H., Wei, W., Ye, G., Jin, S., Jones, A. G., Jing, J., et al. (2014). Three-dimensional Electrical Structure of the Crust and Upper Mantle in Ordos Block and Adjacent Area: Evidence of Regional Lithospheric Modification. *Geochem. Geophys. Geosyst.* 15, 2414–2425. doi:10.1002/2014GC005270
- Duba, A. G., and Shankland, T. J. (1982). Free Carbon & Electrical Conductivity in the Earth's Mantle. *Geophys. Res. Lett.* 9, 1271–1274. doi:10.1029/g1009i011p01271
- Gaillard, F. (2005). Electrical Conductivity of Magma in the Course of Crystallization Controlled by Their Residual Liquid Composition. *J. Geophys. Res.* 110, B06204. doi:10.1029/2004JB003282
- Gaillard, F., Malki, M., Iacono-Marziano, G., Pichavant, M., and Scaillet, B. (2008). Carbonatite Melts and Electrical Conductivity in the Asthenosphere. *Science* 322, 1363–1365. doi:10.1126/science.1164446
- Grigné, C., and Combes, M. (2020). Thermal History of the Earth: On the Importance of Surface Processes and the Size of Tectonic Plates. *Geochem. Geophys. Geosyst.* 21, e2020GC009123. doi:10.1029/2020GC009123
- Guo, H., and Keppler, H. (2019). Electrical Conductivity of NaCl-Bearing Aqueous Fluids to 900 °C and 5 GPa. *J. Geophys. Res. Solid Earth* 124, 1397–1411. doi:10.1029/2018JB016658
- Guo, X., Zhang, L., Su, X., Mao, Z., Gao, X.-Y., Yang, X., et al. (2018). Melting inside the Tibetan Crust? Constraint from Electrical Conductivity of Peraluminous Granitic Melt. *Geophys. Res. Lett.* 45, 3906–3913. doi:10.1029/2018GL077804
- Guo, X., Chen, S., Li, P., Zhang, Y., Wu, X., and Zhang, J. (2020). Phase Transition of Sanidine (KAlSi₃O₈) and its Effect on Electrical Conductivity at Pressures up to 11 GPa. *Phys. Chem. Minerals* 47, 21. doi:10.1007/s00269-020-01089-4
- Hacker, B. R., Sharp, T., Zhang, R. Y., Liou, J. G., and Hervig, R. L. (1997). Determining the Origin of Ultrahigh-Pressure Lherzolites. *Science* 278, 702–704. doi:10.1126/science.278.5338.702
- Hu, H., Dai, L., Li, H., Jiang, J., and Hui, K. (2014). Electrical Conductivity of K-Feldspar at High Temperature and High Pressure. *Miner. Petrol.* 108, 609–618. doi:10.1007/s00710-014-0325-7
- Hu, H. Y., Dai, L. D., Li, H. P., Hui, K. S., and Sun, W. Q. (2017). Influence of Dehydration on the Electrical Conductivity of Epidote and Implications for High Conductivity Anomalies in Subduction Zones. *J. Geophys. Res. Solid Earth* 122, 2751–2762. doi:10.1002/2016jb013767
- Hu, H., Dai, L., Li, H., Sun, W., and Li, B. (2018). Effect of Dehydrogenation on the Electrical Conductivity of Fe-Bearing Amphibole: Implications for High Conductivity Anomalies in Subduction Zones and continental Crust. *Earth Planet. Sci. Lett.* 498, 27–37. doi:10.1016/j.epsl.2018.06.003
- Huang, X., Xu, Y., and Karato, S.-i. (2005). Water Content in the Transition Zone from Electrical Conductivity of Wadsleyite and Ringwoodite. *Nature* 434, 746–749. doi:10.1038/nature03426
- Huang, Y., Guo, H., Nakatani, T., Uesugi, K., Nakamura, M., and Keppler, H. (2021). Electrical Conductivity in Texturally Equilibrated Fluid-Bearing Forsterite Aggregates at 800°C and 1 GPa: Implications for the High Electrical Conductivity Anomalies in Mantle Wedges. *J. Geophys. Res. Solid Earth* 126, e2020JB021343. doi:10.1029/2020JB021343
- Iwamori, H. (1998). Transportation of H₂O and Melting in Subduction Zones. *Earth Planet. Sci. Lett.* 160, 65–80. doi:10.1016/s0012-821x(98)00080-6
- Karato, S. I. (2013). Theory of Isotope Diffusion in a Material with Multiple Species and its Implications for Hydrogen-Enhanced Electrical Conductivity in Olivine. *Phys. Earth Planet. Inter.* 219, 49–54. doi:10.1016/j.pepi.2013.03.001
- Laumonier, M., Farla, R., Frost, D. J., Katsura, T., Marquardt, K., Bouvier, A.-S., et al. (2017). Experimental Determination of Melt Interconnectivity and Electrical Conductivity in the Upper Mantle. *Earth Planet. Sci. Lett.* 463, 286–297. doi:10.1016/j.epsl.2017.01.037
- Li, P., Guo, X., Chen, S., Wang, C., Yang, J., and Zhou, X. (2018). Electrical Conductivity of the Plagioclase-NaCl-Water System and its Implication for the High Conductivity Anomalies in the Mid-lower Crust of Tibet Plateau. *Contrib. Mineral. Petrol.* 173, 16. doi:10.1007/s00410-018-1442-9
- Litasov, K. D., Malkovets, V. G., Kostrovitsky, S. I., and Taylor, L. A. (2003). Petrogenesis of Ilmenite-Bearing Symplectite Xenoliths from Vitim Alkaline Basalts and Yakutian Kimberlites, Russia. *Int. Geol. Rev.* 45, 976–997. doi:10.2747/0020-6814.45.11.976
- Liu, X., Jin, Z., Qu, J., and Wang, L. (2005). Exsolution of Ilmenite and Cr-Ti Magnetite from Olivine of Garnet-Wehrlite. *Sci. China Ser. D-earth Sci.* 48, 1368–1376. doi:10.1360/03yd0590
- Manthilake, G., Bolfan-Casanova, N., Novella, D., Mookherjee, M., and Andrault, D. (2016). Dehydration of Chlorite Explains Anomalous High Electrical Conductivity in the Mantle Wedges. *Sci. Adv.* 2, e1501631. doi:10.1126/sciadv.1501631
- Massonne, H.-J., and Neuser, R. D. (2005). Ilmenite Exsolution in Olivine from the Serpentine Body at Zöblitz, Saxonian Erzgebirge - Microstructural Evidence Using EBSD. *Mineral. Mag.* 69, 119–124. doi:10.1180/0026461056920239
- Ni, H., Keppler, H., and Behrens, H. (2011). Electrical Conductivity of Hydrous Basaltic Melts: Implications for Partial Melting in the Upper Mantle. *Contrib. Mineral. Petrol.* 162, 637–650. doi:10.1007/s00410-011-0617-4
- Pang, K.-N., Li, C., Zhou, M.-F., and Ripley, E. M. (2008). Abundant Fe-Ti Oxide Inclusions in Olivine from the Panzhihua and Hongge Layered Intrusions, SW China: Evidence for Early Saturation of Fe-Ti Oxides in Ferrobasaltic Magma. *Contrib. Mineral. Petrol.* 156, 307–321. doi:10.1007/s00410-008-0287-z
- Parthasarathy, G. (2011). Electrical Properties of Natural and Synthetic Nano-Crystalline MgTiO₃ Geikelite at Mantle Pressure and Temperature Conditions. *Am. Mineral.* 96, 860–863. doi:10.2138/am.2011.3660
- Pearson, D. G., Boyd, F. R., Haggerty, S. E., Pasteris, J. D., Field, S. W., Nixon, P. H., et al. (1994). The Characterisation and Origin of Graphite in Cratonic Lithospheric Mantle: a Petrological Carbon Isotope and Raman Spectroscopic Study. *Contrib. Mineral. Petrol.* 115, 449–466. doi:10.1007/bf00320978
- Poe, B. T., Romano, C., Nestola, F., and Smyth, J. R. (2010). Electrical Conductivity Anisotropy of Dry and Hydrous Olivine at 8 GPa. *Phys. Earth Planet. Interiors* 181, 103–111. doi:10.1016/j.pepi.2010.05.003
- Ponomarenko, A. I. (1977). 1st Find of Garnet-Ilmenite Peridotite with Diamonds from Kimberlite Pipe MIR. *Doklady Akademii Nauk SSSR* 235, 914–917. doi:10.5194/sed-5-1259-2013
- Risold, A.-C., Trommsdorff, V., and Grobety, B. (2003). Morphology of Oriented Ilmenite Inclusions in Olivine from Garnet Peridotites (Central Alps, Switzerland). *Eur. J. Mineralogy* 15, 289–294. doi:10.1127/0935-1221/2003/0015-0289
- Roberts, J. J., and Tyburczy, J. A. (1991). Frequency Dependent Electrical Properties of Polycrystalline Olivine Compacts. *J. Geophys. Res.* 96, 16205–16222. doi:10.1029/91jb01574
- Scambelluri, M., and Philippot, P. (2001). Deep Fluids in Subduction Zones. *Lithos* 55, 213–227. doi:10.1016/S0024-4937(00)00046-3
- She, Y.-W., Song, X.-Y., Yu, S.-Y., and He, H.-L. (2015). Variations of Trace Element Concentration of Magnetite and Ilmenite from the Taihe Layered Intrusion, Emeishan Large Igneous Province, SW China: Implications for Magmatic Fractionation and Origin of Fe-Ti-V Oxide Ore Deposits. *J. Asian Earth Sci.* 113, 1117–1131. doi:10.1016/j.jseas.2015.03.029
- Sun, W., Dai, L., Li, H., Hu, H., Wu, L., and Jiang, J. (2017). Electrical Conductivity of Mudstone (Before and after Dehydration at High P-T) and a Test of High Conductivity Layers in the Crust. *Am. Mineral.* 102, 2450–2456. doi:10.2138/am-2017-6146
- Wang, D., Mookherjee, M., Xu, Y., and Karato, S.-i. (2006). The Effect of Water on the Electrical Conductivity of Olivine. *Nature* 443, 977–980. doi:10.1038/nature05256

- Wang, D., Li, H., Yi, L., Matsuzaki, T., and Yoshino, T. (2010). Anisotropy of Synthetic Quartz Electrical Conductivity at High Pressure and Temperature. *J. Geophys. Res.* 115, B09211. doi:10.1029/2009JB006695
- Wang, D. J., Karato, S. I., and Jiang, Z. T. (2013). An Experimental Study of the Influence of Graphite on the Electrical Conductivity of Olivine Aggregates. *Geophys. Res. Lett.* 40, 2028–2032. doi:10.1002/grl.50471
- Wannamaker, P. E., Caldwell, T. G., Jiracek, G. R., Maris, V., Hill, G. J., Ogawa, Y., et al. (2009). Fluid and Deformation Regime of an Advancing Subduction System at Marlborough, New Zealand. *Nature* 460, 733–736. doi:10.1038/nature08204
- Watson, H. C., Roberts, J. J., and Tyburczy, J. A. (2010). Effect of Conductive Impurities on Electrical Conductivity in Polycrystalline Olivine. *Geophys. Res. Lett.* 37, a–n. doi:10.1029/2009GL041566
- Wirth, R., and Matsyuk, S. (2005). Nanocrystalline (Mg, Fe, Cr)TiO₃ Perovskite Inclusions in Olivine from a Mantle Xenolith, Udachnaya-East Kimberlite Pipe, Siberia. *Earth Planet. Sci. Lett.* 233, 325–336. doi:10.1016/j.epsl.2005.01.023
- Xu, Y., Chung, S.-L., Jahn, B.-m., and Wu, G. (2001). Petrologic and Geochemical Constraints on the Petrogenesis of Permian-Triassic Emeishan Flood Basalts in Southwestern China. *Lithos* 58, 145–168. doi:10.1007/s00410-011-0657-910.1016/s0024-4937(01)00055-x
- Xu, Y., Shankland, T. J., and Poe, B. T. (2000). Laboratory-based Electrical Conductivity in the Earth's Mantle. *J. Geophys. Res.* 105, 27865–27875. doi:10.1029/2000jb900299
- Yamanaka, T., Shimazu, H., and Ota, K. (2001). Electric Conductivity of Fe₂SiO₄-Fe₃O₄ Spinel Solid Solutions. *Phys. Chem. Minerals* 28, 110–118. doi:10.1007/s002690000137
- Yang, X., Keppler, H., McCammon, C., Ni, H., Xia, Q., and Fan, Q. (2011). Effect of Water on the Electrical Conductivity of Lower Crustal Clinopyroxene. *J. Geophys. Res.* 116, B04208. doi:10.1029/2010JB008010
- Yang, X., Keppler, H., McCammon, C., and Ni, H. (2012). Electrical Conductivity of Orthopyroxene and Plagioclase in the Lower Crust. *Contrib. Mineral. Petrol.* 163, 33–48. doi:10.1007/s00410-011-0657-9
- Zhang, Z., Zhi, X., Chen, L., Saunders, A. D., and Reichow, M. K. (2008). Re-Os Isotopic Compositions of Picrites from the Emeishan Flood basalt Province, China. *Earth Planet. Sci. Lett.* 276, 30–39. doi:10.1016/j.epsl.2008.09.005
- Zhang, Z., Mao, J., Saunders, A. D., Ai, Y., Li, Y., and Zhao, L. (2009). Petrogenetic Modeling of Three Mafic-Ultramafic Layered Intrusions in the Emeishan Large Igneous Province, SW China, Based on Isotopic and Bulk Chemical Constraints. *Lithos* 113, 369–392. doi:10.1016/j.lithos.2009.04.023
- Zhang, N., Dygert, N., Liang, Y., and Parmentier, E. M. (2017). The Effect of Ilmenite Viscosity on the Dynamics and Evolution of an Overturned Lunar Cumulate Mantle. *Geophys. Res. Lett.* 44, 6543–6552. doi:10.1002/2017GL073702
- Zhang, Z., and Pommier, A. (2017). Electrical Investigation of Metal-Olivine Systems and Application to the Deep interior of Mercury. *J. Geophys. Res. Planets* 122, 2702–2718. doi:10.1002/2017JE005390

Conflict of Interest: The authors declare that the research was conducted in the absence of any commercial or financial relationships that could be construed as a potential conflict of interest.

Publisher's Note: All claims expressed in this article are solely those of the authors and do not necessarily represent those of their affiliated organizations, or those of the publisher, the editors and the reviewers. Any product that may be evaluated in this article, or claim that may be made by its manufacturer, is not guaranteed or endorsed by the publisher.

Copyright © 2022 Sun, Dai, Hu, Wang, Hu and Jing. This is an open-access article distributed under the terms of the Creative Commons Attribution License (CC BY). The use, distribution or reproduction in other forums is permitted, provided the original author(s) and the copyright owner(s) are credited and that the original publication in this journal is cited, in accordance with accepted academic practice. No use, distribution or reproduction is permitted which does not comply with these terms.